Received: 20 January 2021 | Revised: 1 July 2021 | Accepted: 2 July 2021

DOI: 10.1111/joa.13515

Journal of Anatomy ANATOMICAL SOCIETY WILEY

ORIGINAL PAPER

Association between the developing sphenoid and adult morphology: A study using sagittal sections of the skull base from human embryos and fetuses

Masahito Yamamoto[1] | Zhe-Wu Jin[2] | Shogo Hayashi[3] | José Francisco Rodríguez-Vázquez[4] | Gen Murakami[5] | Shinichi Abe[1]

[1]Department of Anatomy, Tokyo Dental College, Tokyo, Japan

[2]Department of Anatomy, Wuxi School of Medicine, Jiangnan University, Wuxi, China

[3]Department of Anatomy, School of Medicine, International University of Health and Welfare, Narita, Japan

[4]Department of Anatomy and Embryology, School of Medicine, Complutense University, Madrid, Spain

[5]Division of Internal Medicine, Cupid-Fair Clinic, Iwamizawa, Japan

Correspondence
Zhe Wu Jin, Department of Anatomy, Wuxi School of Medicine, Jiangnan University, 1800 Lihu Avenue, Wuxi, Jiangsu, 214122, China.
Email: zwjin@jiangnan.edu.cn

Funding information
Research project of Wuxi Commission of Health, Grant/Award Number: Q201703; Six Talent Peaks Project in Jiangsu Province, Grant/Award Number: SZCY-001

Abstract

The developing sphenoid is regarded as a median cartilage mass (basisphenoid [BS]) with three cartilaginous processes (orbitosphenoid [OS], ala temporalis [AT], and alar process [AP]). The relationships of this initial configuration with the adult morphology are difficult to determine because of extensive membranous ossification along the cartilaginous elements. The purpose of this study was therefore to evaluate the anatomical connections between each element of the fetal sphenoid and adult morphology. Sagittal sections from 25 embryos and fetuses of gestational age 6–34 weeks and crown-rump length 12–295 mm were therefore examined and compared with horizontal and frontal sections from the other 25 late-term fetuses (217–340 mm). The OS was identified as a set of three mutually attached cartilage bars in early fetuses. At all stages, the OS-post was continuous with the anterolateral part of the BS. The BS included the notochord and Rathke's pouch remnant in embryos and early fetuses. The dorsum sellae was absent from embryos, but it protruded from the BS in early fetuses before a fossa for the hypophysis became evident. Although not higher than the hypophysis at midterm, the dorsum sellae elongated superiorly after gestational age 25 weeks. In early fetuses, the AP was located on the side immediately anterior to the otic capsule. The AT developed on the side immediately posterior to the extraocular rectus muscles. At late term, the greater wing was formed by membranous bones from the AT and AP. The AT and AP formed a complex bridge between the BS and the greater wing. A small cartilage, future medial pterygoid process (PTmed) was located inferior to the AT in early fetuses. At midterm, one endochondral bone and multiple membranous bones formed the PTmed. The lateral pterygoid process (PTlat) was formed by a single membranous bone plate. Therefore, we connected fetal elements and the adult morphology as follows. (1) Derivative of the OS makes not only the lesser wing but also the anterior margin of the body of the sphenoid. (2) Derivatives of the BS are the body of the sphenoid including the sella turcica and the dorsum sellae. (3) Most of the greater wing including the foramen rotundum and the foramen oval originate from the AT and AP and multiple membranous bones. (4) The PTmed originate from endochondral bones and multiple membranous bones, while the PTlat derive from a single membranous bone.

KEYWORDS
concha sphenoidalis, human embryo and fetus, membranous bone, pterygoid, sphenoid, Vidian nerve

1 | INTRODUCTION

The sphenoid occupies the center of the skull base, with many cranial nerves passed near or through it. The developing sphenoid has been identified as a median cartilage mass (i.e., the basisphenoid [BS]) with three cartilaginous processes, the orbitosphenoid (OS), the ala temporalis (AT), and the alar process (AP) (Fawcett, 1910; Keibel & Mall, 1910). In these elements, the AP is connected with the AT by a key-and-keyhole structure (Yamamoto et al., 2021), and the internal carotid artery passes between the AP and otic capsule (Honkura et al., 2021). According to Fawcett (1910), the optic nerve is surrounded by the OS, whereas the maxillary nerve penetrates the AT. The OS develops into the lesser wing, and the AT develops into the greater wing (Figure 1). However, the classical concept suggests that, after establishment of the cartilaginous elements, the membranous bones are "newly added" to provide the pterygoid (PT) and most parts of the greater wing. Few studies to date have described the later-developed membranous bones and/or the fetal sphenoid after gestational age (GA) 15 weeks. Moreover, photographic examinations have limited ability to show the topographical anatomy of each element of the developing sphenoid. This has led to a large gap between the classical concept and the actual morphology of the sphenoid in adults.

Gray's Anatomy (Standling, 2005) described the timing and sequence of ossification of multiple elements of the sphenoid. Ossification starts at GA 8 weeks at the root of the greater wing below the foramen rotundum and, at GA 9 weeks, from the lesser wing lateral to the optic canal. At GA 9–10 weeks, membranous bones in the medial PT become ossified, except for the cartilaginous hamulus. At GA 5 months, the concha sphenoidalis, constituting the superoposterior part of the ethmoid, undergoes ossification; before puberty, the concha sphenoidalis fuses with the sphenoid and palatine bones. Finally, at GA 6 months, the lateral and medial parts of the PT join. Those descriptions are applicable to both endochondral and membranous bones in the sphenoid, with both processes proceeding simultaneously, without clear differences in stage and site after 10 weeks. Another section of Gray's Anatomy, however, describes early cartilage elements of the sphenoid (OS, BS, AT, and AP). This situation results in a gap in our understanding of the development and growth of the sphenoid. The purpose of this study was therefore to evaluate the anatomical connections between each element of the fetal sphenoid and adult morphology.

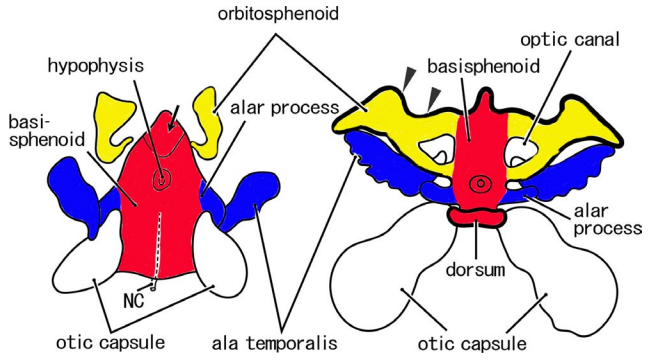

FIGURE 1 Classical view of the cartilaginous sphenoid in human fetuses. Original drawings. Left-hand side, an early stage (an early fetus); right-hand side, a later-stage (a midterm fetus). In the early stage, the cartilaginous sphenoid is composed of four parts: the basisphenoid (BS) (red part), orbitosphenoid (OS) (yellow part), alar process (blue part), and ala temporalis (blue part). The OS does not surround the optic nerve completely. The anterior end of the BS is similar to the adult morphology (arrow). In the later-stage, the entire anterior margin of the OS (arrowheads) fuses with the ethmoid. The dorsum sellae (dorsum) is established. NC, notochord

2 | MATERIALS AND METHODS

This study was conducted in accordance with the principles of the Declaration of Helsinki 1995 (as revised in 2013). Paraffin-embedded sagittal sections were obtained from 25 embryos and fetuses of approximate GA 6–34 weeks and CRL 12–295 mm. Because sagittal sections show topographical anatomy better than horizontal sections, sagittal sections of the sphenoid have been used to assess the anatomy of the developing cavernous sinus (Sato et al., 2020) and extraocular rectus muscles (Kim et al., 2020; Naito et al., 2019). The specimens were categorized into four groups by age and size, with Group 1 consisting of four embryos of GA 6 weeks and CRL 12–15 mm, Group 2 of six early fetuses of GA 7–8 weeks and CRL 24–35 mm, Group 3 of eight midterm fetuses of GA 12–15 weeks and CRL 71–115 mm, and Group 4 of seven late-term fetuses of GA 25–34 weeks and CRL 200–295 mm. All sections were part of the large collection kept at the Department of Anatomy of the Universidad Complutense, Madrid, and were the results of miscarriages and ectopic pregnancies from the Department of Obstetrics of the University. Sections of the embryos, early fetuses, and midterm fetuses had been prepared serially, whereas the late-stage fetuses had been sectioned at 50 or 100 μm intervals. The sections were stained with hematoxylin and eosin (HE) or Azan. The study protocol was approved by the Ethics Committee of Complutense University (B08/374).

Most photographs were taken with a Nikon Eclipse 80, whereas photographs at ultra-low magnification (objective lens less than ×1) were obtained using a high-grade flat scanner with translucent illumination (Epson scanner GTX970). In addition to the sagittal

sections from 25 specimens, structures requiring identification were assessed by reexamining photographs of horizontally or frontally sectioned sphenoids taken for previous studies (Cho et al., 2010, 2013; Honkura et al., 2017; Jin et al., 2011; Katori, Kawamoto, et al., 2013; Katori, Kawase, et al., 2013; Kim et al., 2020; Kiyokawa et al., 2012; Osanai et al., 2011; 2011, 2017; Yamamoto et al., 2017, 2018). In these previous specimens, horizontal and frontal sections from 25 late-term fetuses (GA 28–40 weeks and CRL 217–340 mm; Kim et al., 2020) were especially useful for detailed understanding of topographical anatomy. Therefore, the observations will be added in the final subsection of the results with figure demonstration of two of the 25 specimens.

3 | RESULTS

Table 1 lists the major structures in and near the sphenoid that are shown in Figures 2–8; these structures include Rathke's pouch, the notochord, the cranial nerve, and its associated ganglion, and the internal carotid artery. Table 1 does not include the maxillary and mandibular nerves shown in Figure 9 because these nerves appear easy to identify. A description of the initial sphenoid sinus is limited to Figure 9 because an epithelial pouch for the sinus appeared at late-term and approached the anterior margin of the BS. The panels from left to right in all of these figures are arranged from the medial site to the lateral site; in each panel, the right-hand side corresponds to the anterior site of the skull base. Thus, from the right-hand side of panel A to the left-hand side of the final panel, multiple elements of the sphenoid are usually shown in the following order: the OS, the BS, the medial part of the pterygoid (PTmed), the AP, the AT, and the lateral part of the pterygoid (PTlat). The topographical anatomy of the skull base is shown at lower magnification in Figures 4, 7, and 8.

3.1 | The BS and the hypophyseal fossa

The notochord and Rathke's pouch remnant were almost always found in the BS (indicated by red color in the figures) in embryos and early fetuses (Figures 2a,b, 3a,b, and 4a), but they were difficult to detect in midterm fetuses. The notochord started from the pharyngeal aspect of the BS, ran superiorly, and ended at the center of the BS on the slightly posterior side of the Rathke's pouch remnant. The dorsum sellae was absent from embryos (Figures 2c and 3a), but it protruded from the BS near the notochord terminal in early fetuses before a fossa for the hypophysis became evident (Figure 4a). Although not higher than the hypophysis at midterm (Figure 7a), the dorsum sellae elongated superiorly after GA 25 weeks (Figure 8a). Except in a few specimens (data not shown), the anterior and posterior clinoid processes were not evident even in late-term fetuses. The long cartilage bars extending anteriorly were not the clinoid but the OS paramedian part (Figures 6a and 8a). The BS and basioccipital became continuous by GA 25 weeks, with the initial syndesmosis appearing as eosinophilic homogeneous tissue without a joint space.

Anteriorly, the BS in embryos was widely fused with the nasal capsule (strictly, the initial ethmoid including the nasal septum), with a border between them becoming evident at GA 7–8 weeks (Figure 4b). However, depending on enlargement of the orbital content and nasal cavity at midterm, the BS-ethmoid attachment became restricted to the midsagittal area (a connection between the BS and nasal septum). In the paramedian area, the OS was located on the anterior side of the BS, whereas the ethmoid occupied the inferior rather than the anterior side of the OS (Figures 6a, 7a, and 8a). At late-term, the paramedian area contained an initial sphenoid sinus, with an epithelial pouch from the posterior roof of the nasal cavity surrounded by the bony plates of the ethmoid (Figure 9e–g). Ossification of the nasal capsule cartilage,

TABLE 1 A guidance as to which figure shows a cranial nerve passing through the sphenoid and photos showing cranial base ganglia and other major structures

	Figure 2	Figure 3	Figure 4	Figure 5	Figure 6	Figure 7	Figure 8
Optic nerve (I)	–	DE	E	B	C	B	C
Oculomotor nerve (III)	E	F	G	D	E	D	DE
Ophthalmic nerve (V1)	I	H	G	F	G	–	–
Maxillary nerve (V2)	J	I	H	H	H	F	F
Mandibular nerve (V3)	I	J	I	J	J	H	I
Vidian nerve	F	F	E	C	D	CD	A
Ciliary ganglion	G	G	H	F	–	E	–
Pterygopalatine ganglion	HI	GH	EF	CD	D	C	C
Otic ganglion	H	I	I	H-J	I	H	HI
Geniculate ganglion	G	J	H	–	–	–	–
Internal carotid artery	D	F	E	E	E	E	D
Rathke's pouch	A	AB	A	–	–	–	–
Notochord	B	B	A	A	–	–	–

A–J, panel in the figure.

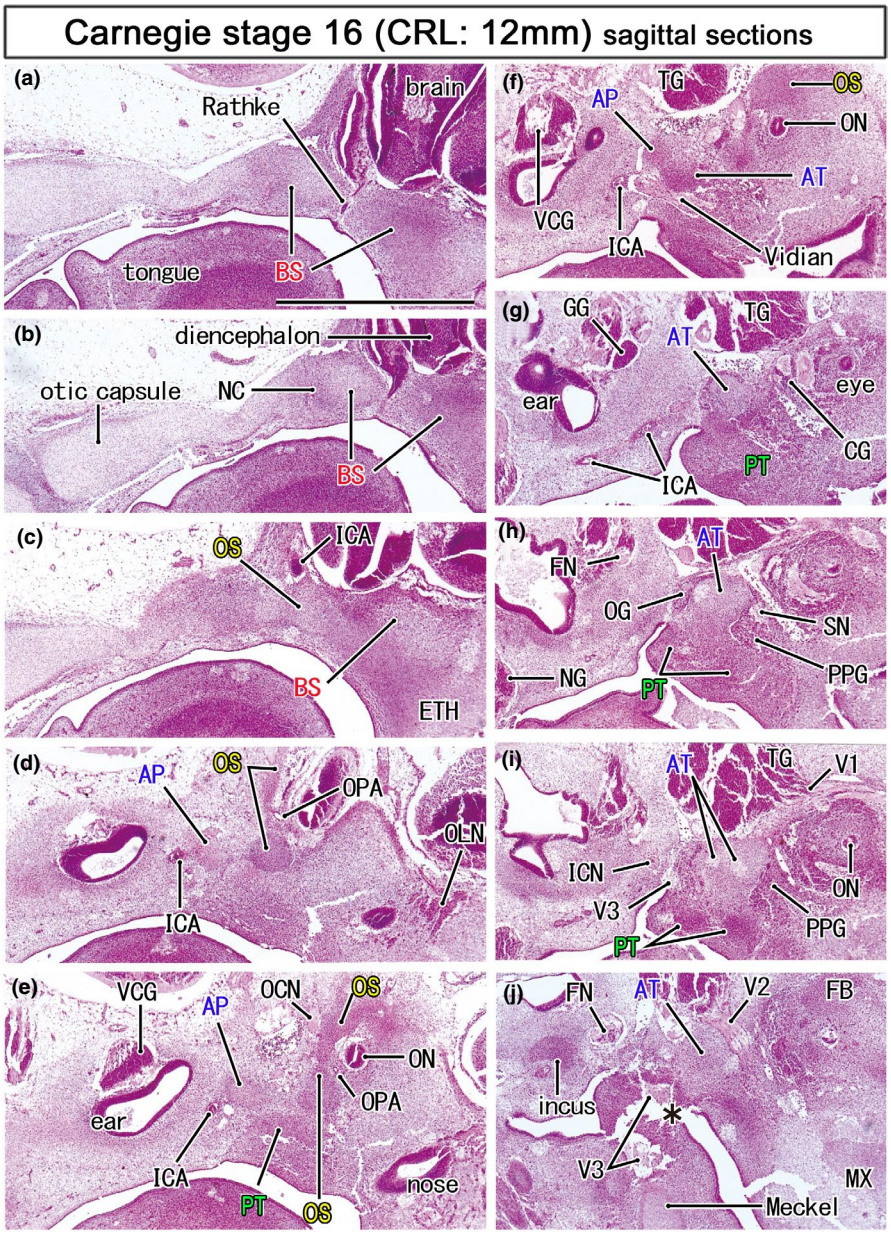

FIGURE 2 Mesenchymal condensations for the initial sphenoid in embryos of 12 mm CRL. HE staining. Left-hand side of each panel corresponds to the posterior site. Panel (a) displays the most medial site in the figure, while panel (J) the most lateral. The initial sphenoid was identified as five mesenchymal condensations: (1) the basisphenoid (BS; panels a–c) containing the Rathke's pouch (Rathke) and notochord (NC), (2) the orbitoshpenoid (OS) protruding superiorly (panels d and e), (3) the alar process (AP) near the developing inner ear (panels e and f) and, (4) the ala temporalis (AT), and (5) the pterygoid in the inferolateral side of the Vidian nerve (panels f and g). The sphenoid nerve (SN; panel h) transiently connects between the otic and pterygopalatine ganglia. All panels are prepared at the same magnification (scale bar in panel a, 1 mm). Other abbreviations, see the common abbreviation

comprised of the ethmoid and others, started at GA 25 weeks. Parts of the ethmoid around the sinus did not fuse with the BS even at GA 34 weeks because of the underdeveloped concha sphenoidalis. Notably, there were inter-individual variations among the bones surrounding the initial sinus. A large bony mass on the inferior side of the sinus corresponded to the posterior end of the ethmoid (Figure 9e) or the anterior end of the vomer (Figure 9f,g). The palatine bone (Figure 9g) or the PT-med (Figure 9e) was located on the posterolateral side of the vomer.

3.2 | The OS and the orbital apex

The OS (indicated by yellow color in the figures) was identified as a set of three mutually attached cartilage bars: the anterior (OSant), posterior (OSpost), and superior (OSsup) cartilage bars. These cartilages were present 0.2–0.8 mm to the anterior side of Rathke's pouch remnant. At all stages, the OSpost was continuous with the anterolateral part of the BS (Figures 3d, 4c, 5b, 6b, and 7b). The initial morphology of the optic canal consisted of the OSant

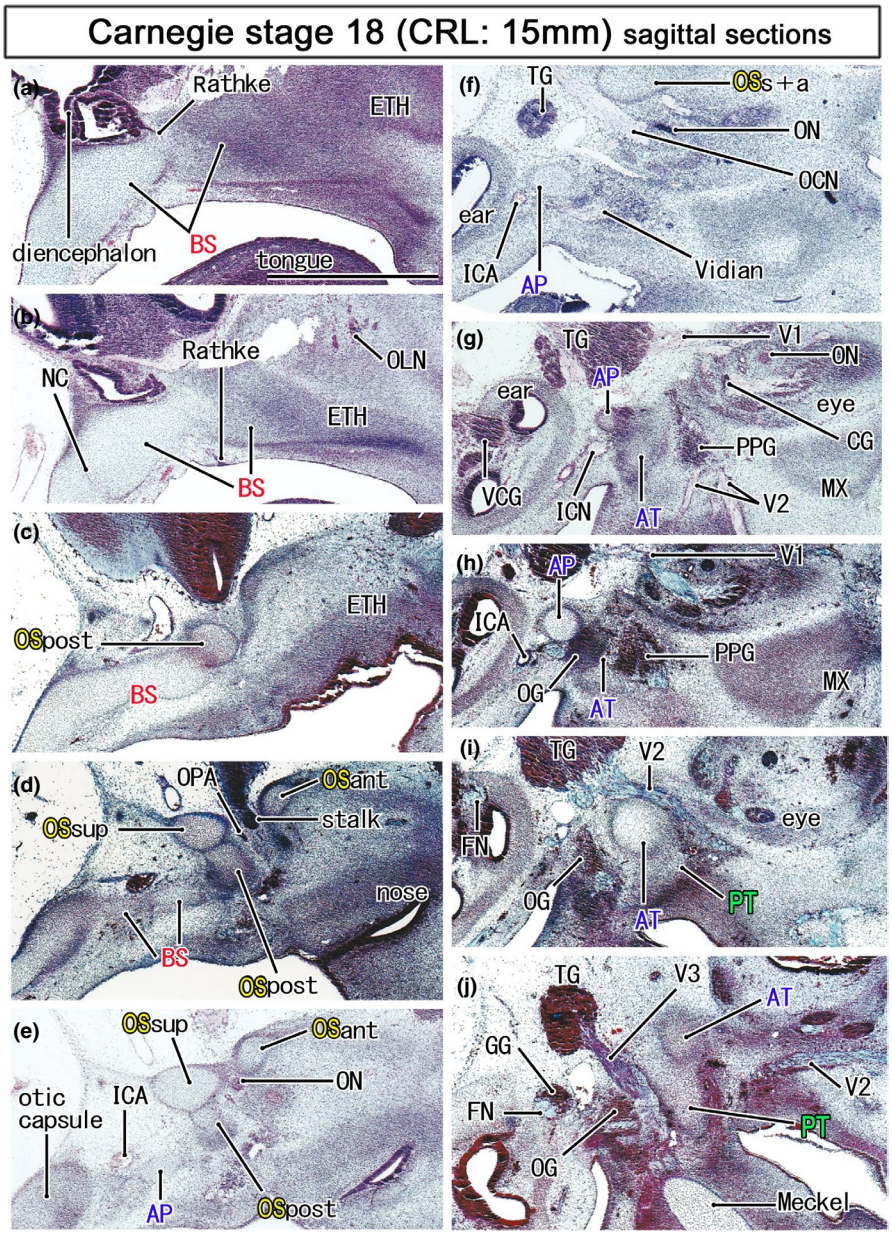

FIGURE 3 Initial cartilages of the sphenoid in embryos of 15 mm CRL. Azan staining. Left-hand side of each panel corresponds to the posterior site. Panel a displays the most medial site in the figure, while panel (j) the most lateral. The notochord is not contained in this figure. The orbitosphenoid (OS) is composed of the posterior, anterior and superior cartilage bars (OSpost, OSant, and OSsup) and they surround the optic nerve and ophthalmic artery (ON, OPA; panels d and e). The OSpost is attached to the basisphenoid (BS), while the OSsup and OSant joins in lateral sections (OSsup+ant in panel f). The pterygoid (PT) is still a mesenchymal condensation (panel j). All panels are prepared at the same magnification (scale bar in panel a, 1 mm). Other abbreviations, see the common abbreviation

and OSpost sandwiching the optic nerve until GA 7–8 weeks. In contrast, the OSsup was attached to the superior aspect of the OS post. The OSsup and OSant subsequently became fused (OSant+sup) on the lateral side of the optic canal, providing a cartilage plate that reached the initial frontal bone (Figures 3f and 4f). After GA 25 weeks, however, another short cartilage plate was found to extend anteriorly from the bony OSant+sup on the upper aspect of the frontal bone, with this plate riding over the frontal bone (Figure 9c). Although the OSpost was much smaller than the OSant+sup at midterm (Figures 6d and 7d), the OSpost fused with the BS to provide a large median mass of the sphenoid by GA 25 weeks (Figure 8b), providing a limited connection between the definite greater and lesser wings. At the orbital apex, the OSpost was separated from the AT by veins. Similarly, the OS was distant from the maxilla or future inferior margin of the orbital fissure (Figure 8c,d). The orbital muscle was not attached to the OSpost but connected the maxilla and a membranous bone from the AT (Figures 6j, 7f, and 8g). At late-term, the orbital apex appeared to be closed by a fibrous tissue (Figure 9b,d), but this tissue plug was located far laterally to the large orbital fissure.

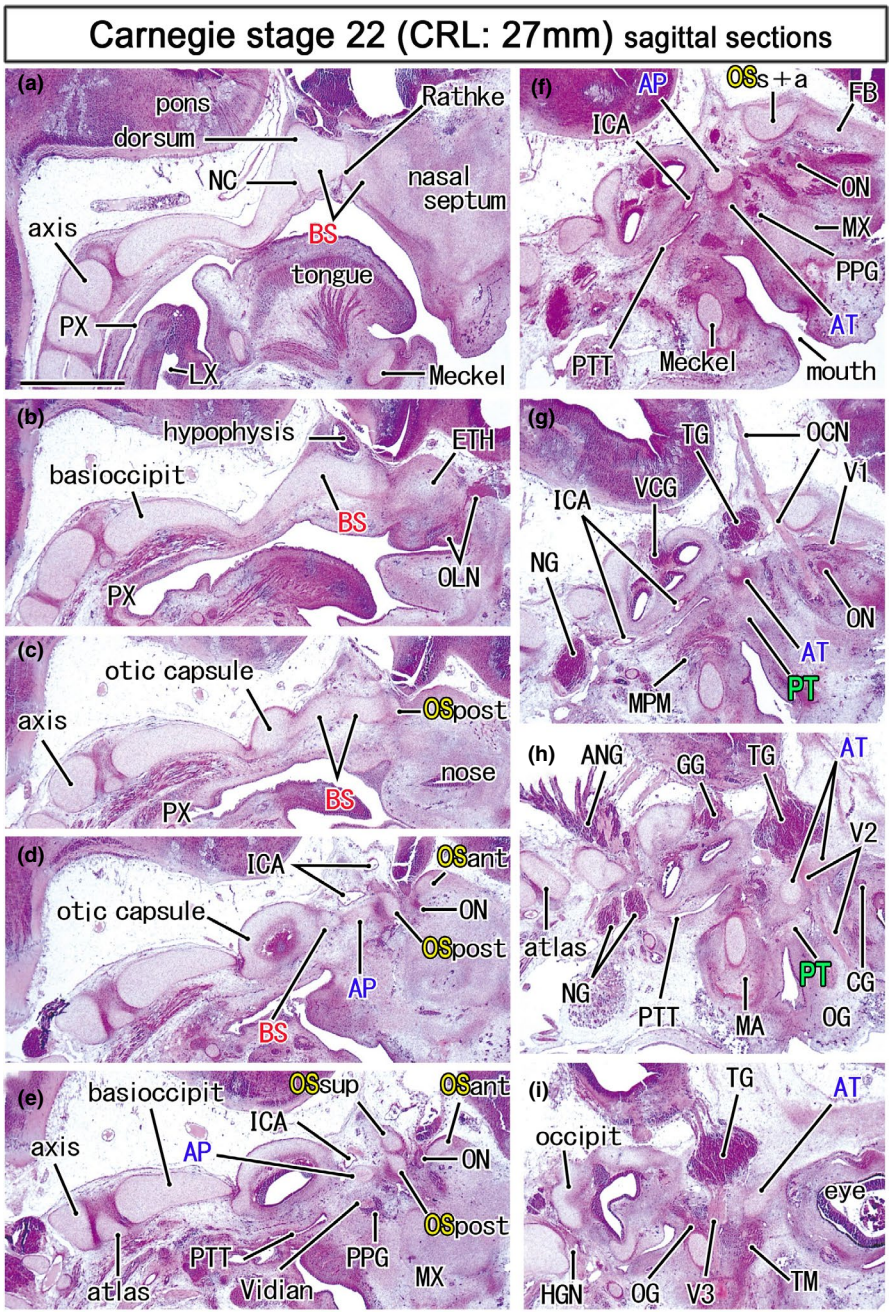

FIGURE 4 Topographical anatomy of the skull base in an early fetus (27 mm). HE staining. Panel (a) displays the most medial site in the figure, while panel (i) the most lateral. Left-hand side of each panel corresponds to the posterior site. Behind the hypophysis (panels a and b), a posterior protrusion of the basisphenoid (BS) is identified as the dorsum sellae (dorsum). Three cartilages of the OS (OSsup, OSpost, OSant) surrounds the optic nerve (ON; panel e). The oculomotor nerve (OCN) passes below the union of the OSsup and OSant of the OS (OSs+a; panel f). The maxillary nerve (V2) passes through the ala temporalis (AT; panels h). All panels are prepared at the same magnification (scale bar in panel a, 1 mm). Other abbreviations, see the common abbreviation

After GA 7 weeks, the OS-post delineated the superomedial margin of the large orbital fissure, forming the posterolateral wall of the optic canal, extending laterally, and approaching the anterosuperior end of the AT, which was the future lateral wall of the fissure (Figures 7c,d and 8c,d). The courses of the oculomotor and trochlear nerves to the target immediately below the OS-post were almost straight (Figures 4g and 6e). Due to the underdevelopment of membranous bones from the AT, the orbital fissure, even at GA 34 weeks, opened widely to the large pterygopalatine fossa and parasellar area. The former fossa was present between the maxilla and AT, whereas the latter area was surrounded by the BS, OS, and AT (Figure 8d,e). The OS-post provided the origins of the inferior and medial rectus muscles (Figures 5c, 6d, 7c,d, and 8c,d), whereas the superior obliquus was found to originate from the OS-sup and/or OS-ant (Figures 6c, 7b, and 8c).

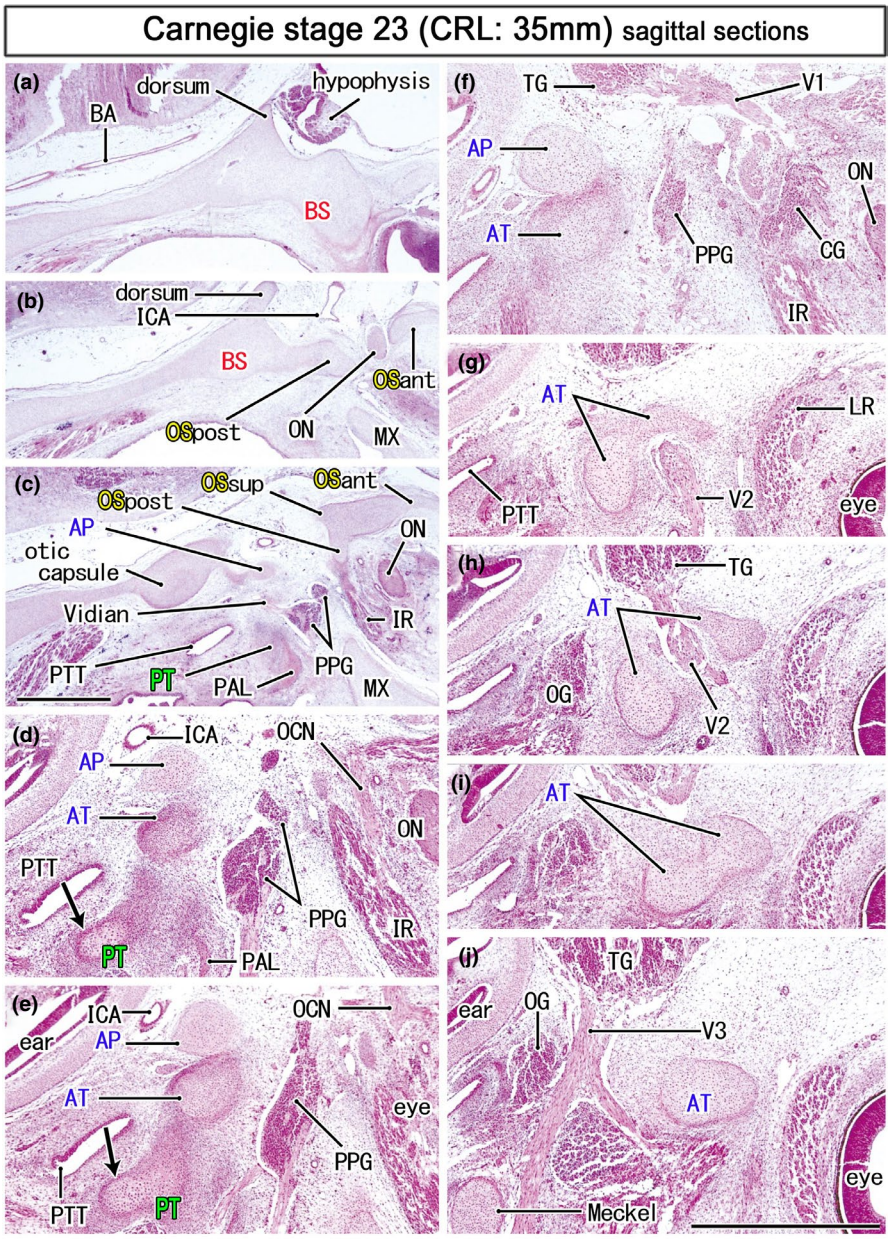

FIGURE 5 Ala temporalis and the maxillary nerve in an early fetus (35 mm). HE staining. Panel (a) displays the most medial site in the figure, while panel (j) the most lateral. Panels (d–j) were prepare at a magnification higher than panels a–c (scale bars in panels c and j, 1 mm). Left-hand side of each panel corresponds to the posterior site. Three cartilaginous of the OS (OSand, OSpost, OSsup) surrounds the optic nerve (ON; panel b) and they join to provide a posterior part of the orbital roof (panel c). The maxillary nerve (V2) passes through the cartilaginous ala temporalis (AT; panels g–i). A mesenchymal condensation for the pterygoid (PT) contains a cartilage mass (arrows in panels d and e) than extends along the pharyngotympanic tube (PTT). All panels are prepared at the same magnification (scale bar in panel a, 1 mm). Other abbreviations, see the common abbreviation

3.3 | The AT, AP, and definite greater wing

In embryos, a mesenchymal condensation of the AP (indicated by blue color in the figures) was found on the superior side of the condensation of the AT (indicated by blue color in the figures) (Figure 2f). As previously reported (Yamamoto et al., 2018), the early AT appeared to divide a single large ganglion into the pterygopalatine and otic ganglia, with the PT nerve transiently communicating between these two ganglia (Figures 2h and 3g,h). The supero-inferior topographical relationship between these two cartilage bars was maintained in early fetuses (Figures 3g, 4f, and 5e). Because the AT was much larger than the AP until midterm, the AP became a small postero-superior protrusion of the AT at midterm (Figures 6e,f and 7e,f). At midterm, bones at multiple stages of endochondral ossification were present in the AT (Figure 7e,f). At late term, the bony AP was inserted deeply into a cartilaginous core of the AT (Figure 8e). A connection between the BS and AP was difficult to detect in sagittal sections (Figure 5c; see also the final subsection of the Section 3).

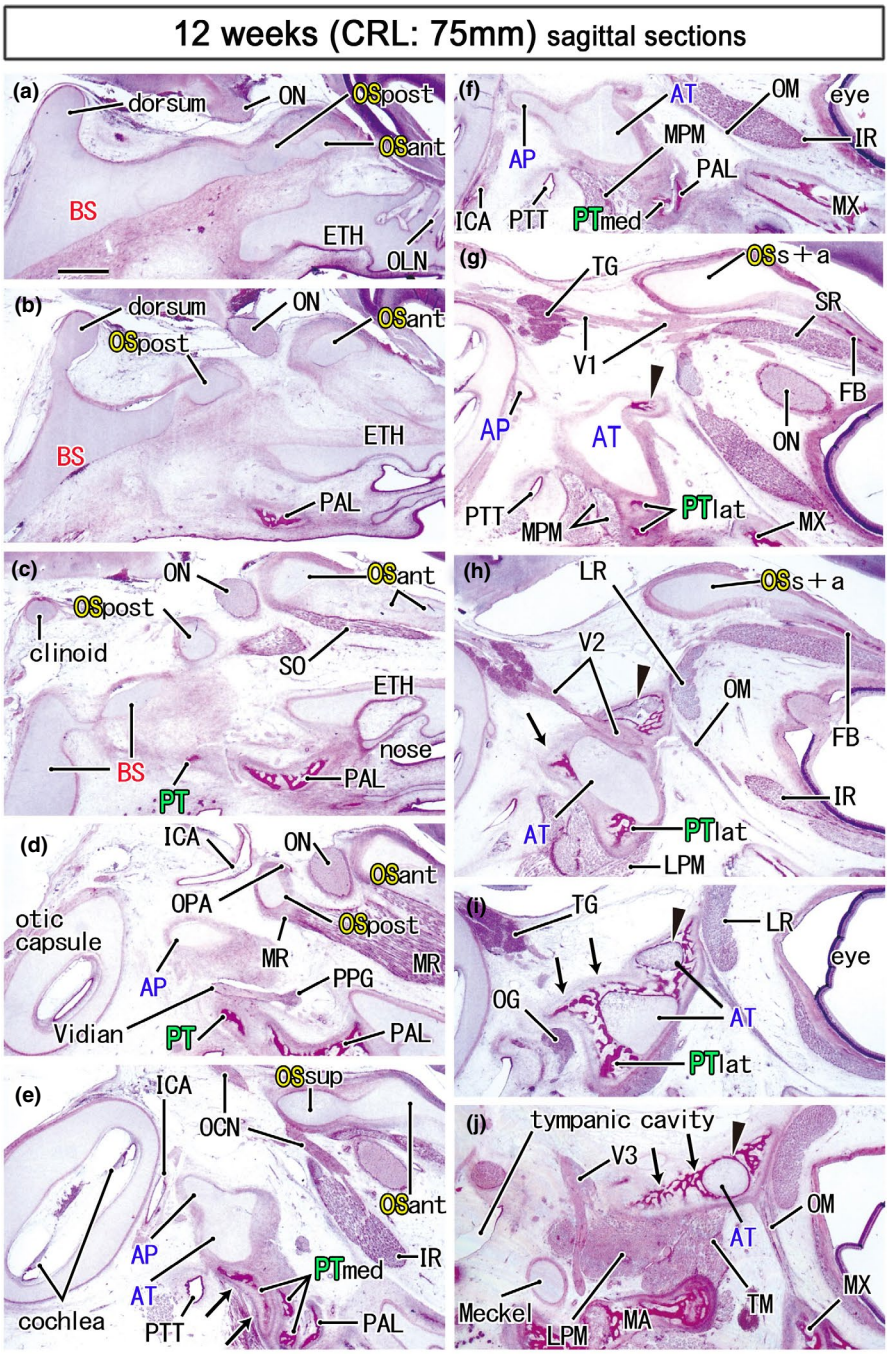

FIGURE 6 Ossification in the sphenoid and nearby bones in a midterm fetus (75 mm). HE staining. Panel (a) displays the most medial site in the figure, while panel (j) the most lateral. Left-hand side of each panel corresponds to the posterior site. The anterior part of the OS (OSant) extends anteriorly (panels a–e) and meets the bony frontal bone (FB; panels g and h). Ossification in the cartilaginous ala temporalis (arrowhead in panels g–j) makes a mosaic of bone and cartilage around the maxillary nerve (V2). Notably, the medial part of the pterygoid (PTmed) contains a cartilaginous bone (arrows in panel e). In the lateral side of the palatine bone (PAL), membranous bones in the lateral part of the pterygoid (PTlat; panels g and h) continue to the ala temporalis (arrows in panels h–j). The medial pterygoid muscle (MPM) attaches to not only the pterygoid but also to the ala temporalis (panels f and g). All panels are prepared at the same magnification (scale bar in panel a, 1 mm). Other abbreviations, see the common abbreviation

The AP developed on the side immediately anterior to the otic capsule or internal ear, whereas the AT developed on the side immediately posterior to the extraocular rectus muscles. After GA 7 weeks, the AP was separated from the otic capsule or the temporal bone petrosal portion by the internal carotid artery (Figures 3h, 5e, 7e, and 8d). Likewise, in embryos, the AT was separated from the extraocular muscle by the maxillary nerve or the pterygopalatine ganglion (Figures 2j and 3i). Even in embryos, however, the maxillary nerve passed through the cartilaginous AT. The cartilaginous foramen rotundum was clearly seen at GA 8 weeks (Figure 5g–i). The marked upward and lateral

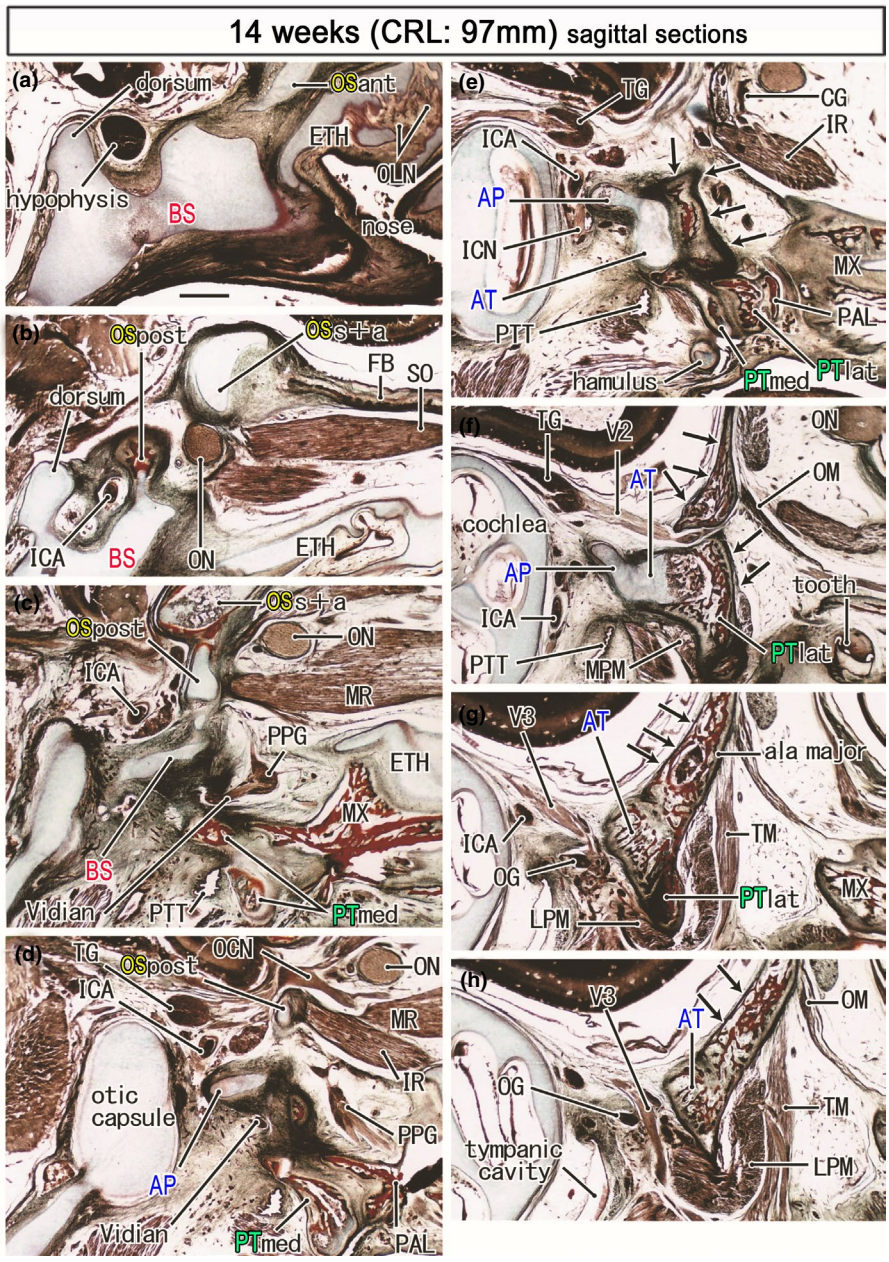

FIGURE 7 Ossified pterygoid and the upper growth of the bony ala major in a midterm fetus (97 mm). Azan staining. Panel (a) displays the most medial site in the figure, while panel (h) the most lateral. Left-hand side of each panel corresponds to the posterior site. The bony frontal bone extends posteriorly to meet the supero-anterior part of the OS (OSs+a; panel b). The medial and inferior rectus muscles (MR, IR) originate from the posterior part of the OS (OSpost in panels c and d). The pterygoid (PTmed, PTlat) is ossified except for the hamulus (panel e). Membranous bones of the greater wing (ala major; arrows in panels e–h) extend along the posterior aspect of the ala temoralis and continue to lateral part of the pterygoid (panels f and g). All panels are prepared at the same magnification (scale bar in panel a, 1 mm). Other abbreviations, see the common abbreviation

growth of the AT, due to additional membranous bones at and after midterm (Figures 6h and 7f), resulted in the AT forming the postero-lateral wall of the orbit and approaching the orbital roof. Posteriorly, a membranous bone from the AP formed the foramen ovale after GA 25 weeks (Figure 8h,i). During late-term, however, the superoposterior marginal parts of the greater wing were not attached to the bony squamosal parts of the temporal, parietal, and frontal bones.

Consequently, all parts of the definite greater wing were formed by membranous bones from the AP and AT after GA 12 weeks. The AP and AT formed a complex bridge between the BS and the later-developed greater wing. However, the present sagittal sections did not demonstrate details of the complex (see the final subsection of Section 3). In addition, a candidate for the lingula sphenoidalis was not seen. Instead of the lingula, a membranous bone from the AP provided the anterosuperior wall of the carotid canal (Figure 9a). At late-term, the future cavernous sinus was surrounded by the BS, OSpost, AP, and the petrosal portion of the temporal bone (Figure 8a–d). The intracavernous course of the carotid artery was almost straight.

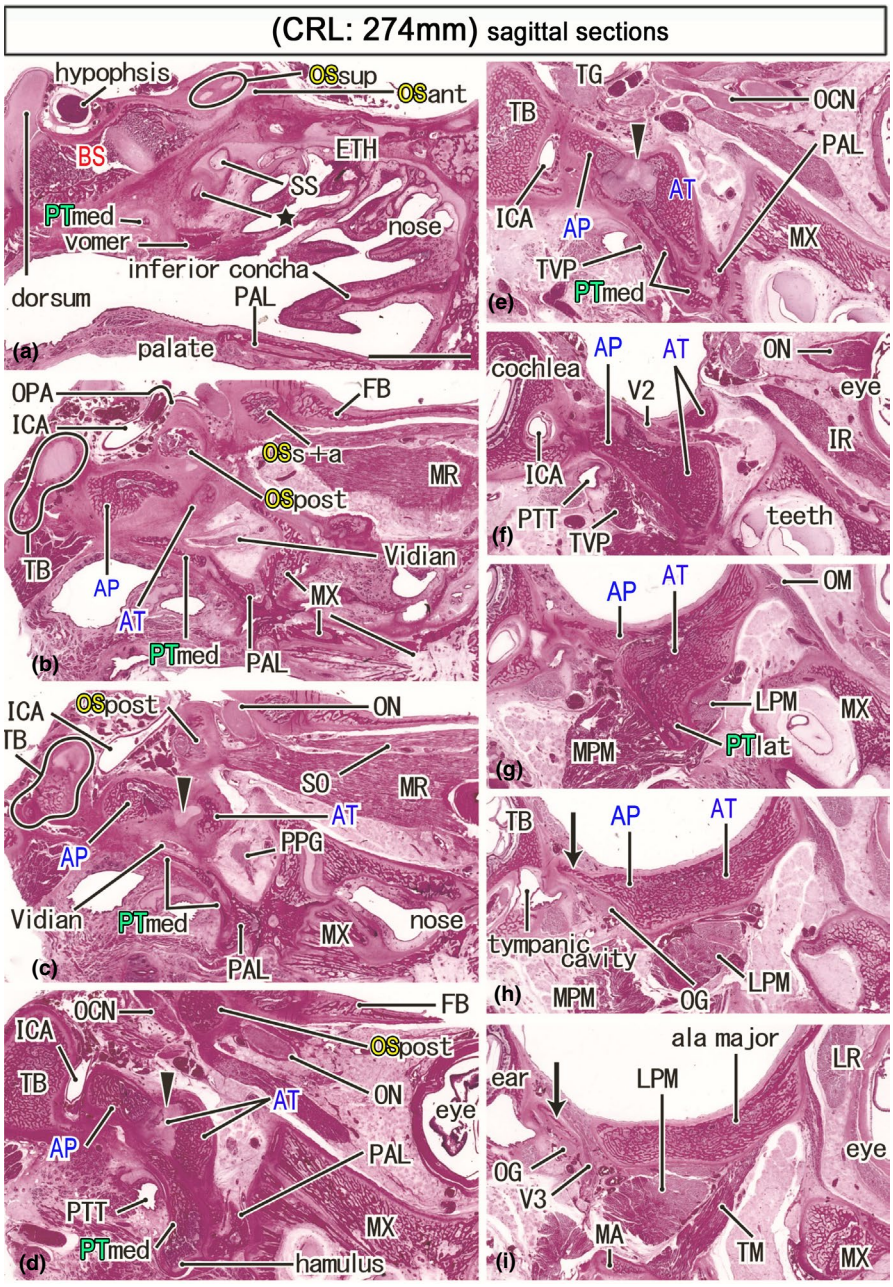

FIGURE 8 Ossified sphenoid in a late-term fetus (274 mm) that suggests the morphology at birth. HE staining. Panel (a) displays the most medial site in the figure, while panel (i) the most lateral. Left-hand side of each panel corresponds to the posterior site. A posterior end of the ethmoid (ETH) is ossified (star in panel a) below the initial sphenoid sinus (SS). A large part of the orbital roof is made by the frontal bone (FB; panel b), while ossification of the OS is limited to the optic canal (OSs+a, OSpost; panels b and c) and the superior wall of the orbital fissure (OSpost; panel d). The bony alar process (AP) faces the internal carotid artery (ICA; panels d and e). The lateral part of the pterygoid (PTlat) is identified as a mere inferior protrusion of the ala temporalis (panel g). A membranous bone (arrows in panels h and i), possibly originating along the AP, surrounds the mandibular nerve (V3). All panels are prepared at the same magnification (scale bar in panel a, 10 mm). Other abbreviations, see the common abbreviation

3.4 | The PT and the muscles surrounding it

The PT (indicated by green color in the figures) in embryos and early fetuses was identified as a mesenchymal condensation surrounded by the AT, pterygopalatine ganglion, and mandibular nerve (Figure 3i,j). In early fetuses, a cartilage bar was observed in the medial part of the condensation below the cartilaginous AT (Figure 5d,e). Ossification of the PT began earlier than ossification of the other parts of the sphenoid (Figures 6e and 7c,d); at midterm, one endochondral bone and multiple membranous bones formed the medial pterygoid (PTmed) (Figures 6e and 7d), with the cartilaginous hamulus connected to the PTmed. The lateral pterygoid (PTlat), located on the anterolateral side of the PTmed and the ossified palatine bone, was formed by a single membranous

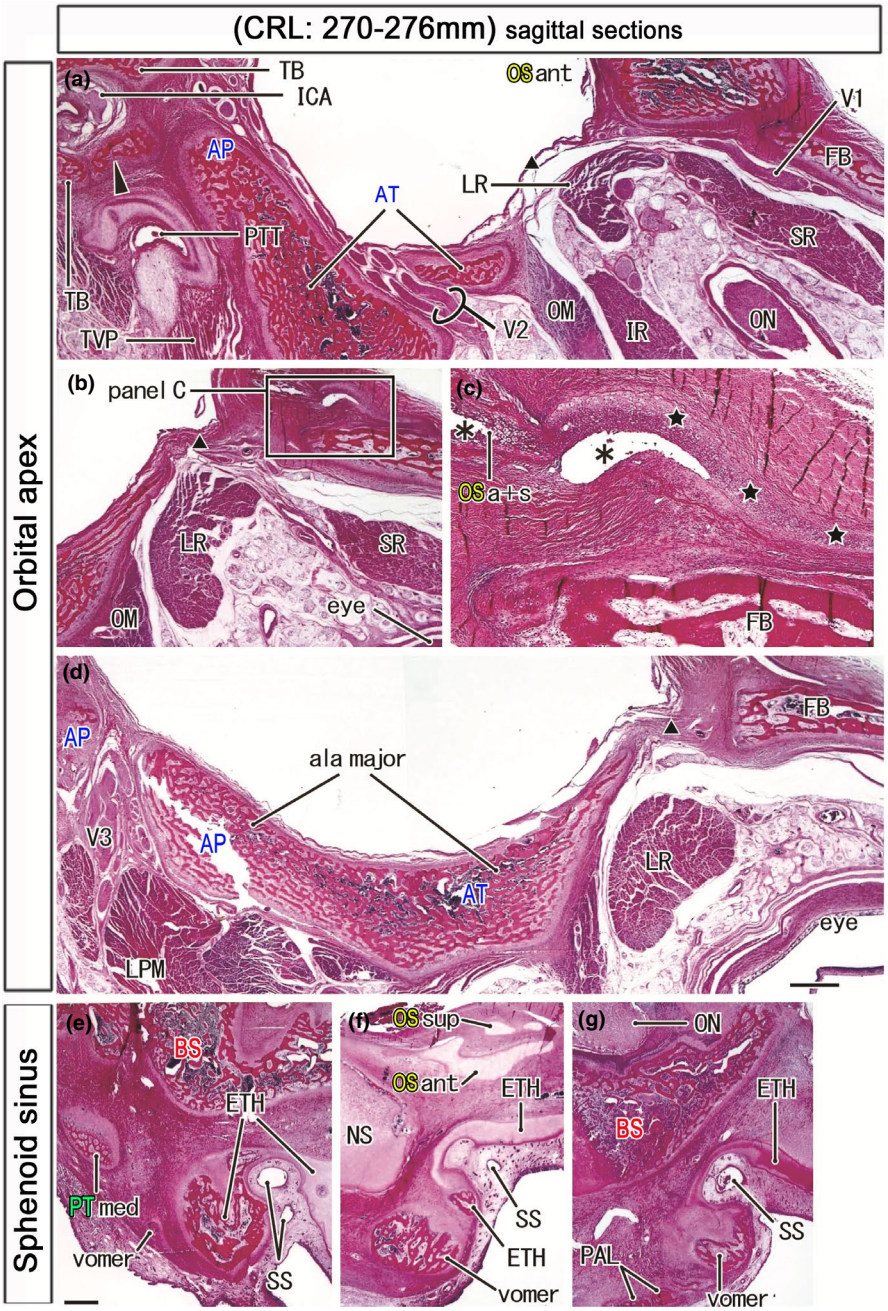

FIGURE 9 Orbital apex and the sphenoidal sinus in late-term fetuses. HE staining. Left-hand side of each panel corresponds to the posterior site. Panels a–d (a fetus of 270 mm CRL) display the orbital apex. Panel (c) is a higher magnification view of a square in panel (b). Panel (a) shows the most medial site in the fetus. A membranous bone from the alar process along the internal carotid artery (arrowhead in panel (a)) provided the anterosuperior wall of the bony carotid canal. The OS has a cartilaginous process (stars in panel c) extending anteriorly on the frontal bone. Asterisks indicate artifact spaces during histological procedure. The expanding greater wing (ala major) was not contact with the frontal bone (FB) and orbitosphehnoid (OSa+s) but interposed by a fibrous tissue (triangle in panels a, b, and d). Panel (e) (270 mm CRL), panel (f) (274 mm), and panel (g) (276 mm) exhibit an individual variation in bony components around the initial sphenoid sinus (SS). A large bony mass corresponds to a posterior end of the ethmoid (ETH; panel e) or an anterior end of the vomer (panels f and g). The palatine bone (PAL; panel g) or the medial part of the pterygoid (PTmed; panel e) is in the posterior side of the vomer. Panels a, b, and d (or panels e–f) are prepared at the same magnification (scale bars in panels A, C, and E, 1 mm). Scale bar in panel c is 1 mm. Other abbreviations, see the common abbreviation

bone plate covering the anterior and inferior aspects of the cartilaginous AT (Figures 6h,i and 7e,f). No clear border was observed between the PTlat and other membranous bones for the future greater wing.

The Vidian nerve was found to pass below the early AP or AT (Figures 2f, 3f, and 4e), but the topographical relationship of this nerve to the PT was difficult to determine because a limited cartilage element of the PT was still far lateral to the nerve

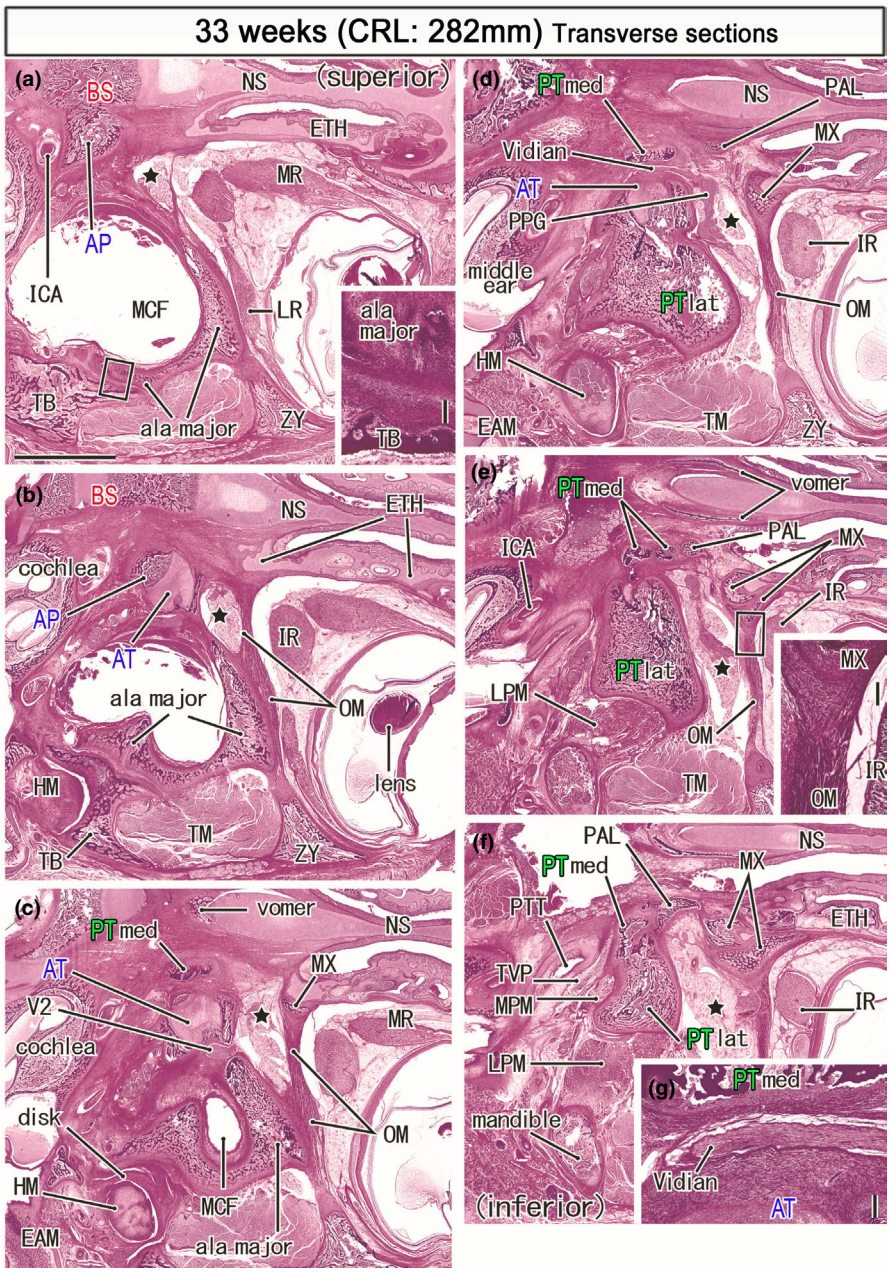

FIGURE 10 Horizontal sections of a specimen at 33 weeks (282 mm CRL). Panel (a) displays the uppermost section, while panel (f) the lowermost. Intervals between panels are 0.8 mm (a, b), 0.7 mm (b, c), 0.6 mm (c, d), 0.5 mm (d, e) and 0.7 mm (e, f). The bony alar process (AP) connects to the basisphenoid (a) medially and the ala temporalis laterally (AT; panel b). A bulky membranous bone of the greater wing (ala major) faces the zygomatic bone (ZY; panel a), the squamous portion of the temporal bone (TB; panels a and b), and a disk of the temporomandibular joint (panels c). The PT-med carries the top in panel (c), faces the Vidian nerve in panel (d), divides into four pierces in panel (e) and, attaches to the PT-lat in panel (f). The orbital muscle (OM) extends from the greater wing to the ethmoid (ETH; panel b) and the maxilla (MX; panels c). The smooth muscle also extends between the maxilla and zygomatic bone (panels d and e). The pterygopalatine fossa (star) is large and separated from the orbit by the orbital muscle (OM). Panel (g) shows a higher magnification view of the Vidian nerve in panel (d). Insert in panels (a) and (e) corresponds to a square in the panel, respectively. Panels (a–f) are prepared at the same magnification (scale bar: 5 mm in panel (a); 0.2 mm in two inserts and panel (g). Other abbreviations, see the common abbreviation

(Figure 5c,d). After GA 12 weeks, the nerve was clearly identified between a membranous bone of the PT-med and the cartilaginous AT (Figures 6d, 7c, and 8c). The anterior part of the nerve was likely to face the palatine bone and/or vomer. The pharyngotympanic tube was located on the posterior side of the PTmed, but it was also near and below the AT at all stages. The initial temporalis muscle, which connected the AT and the membranous bone of the mandible (Figure 4h,i), originated from membranous bones along the AT at midterm (Figures 6j and 7g). The lateral PT muscle was attached to or surrounded the membranous bones of the

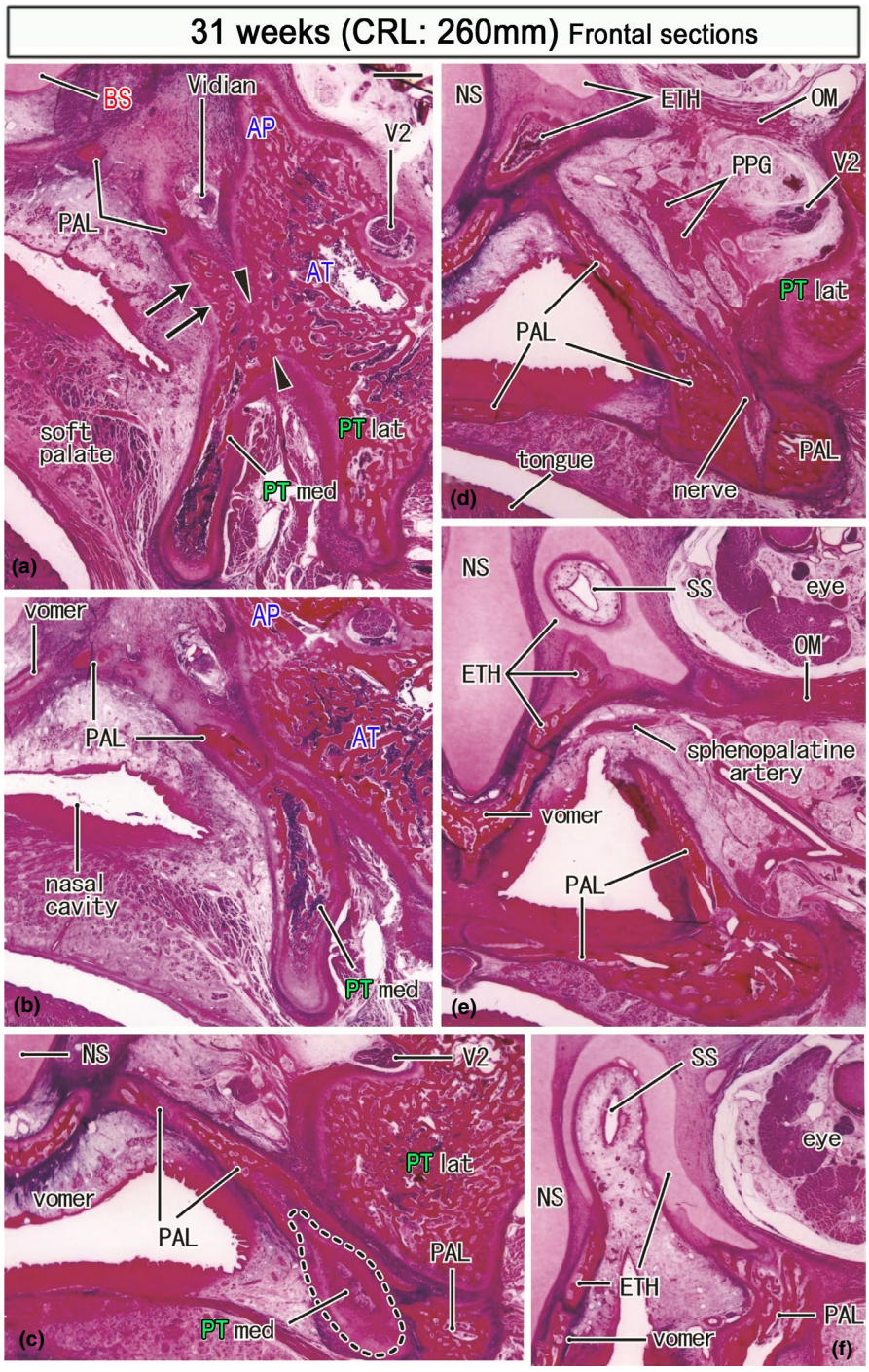

FIGURE 11 Frontal sections of a specimen at 31 weeks (260 mm CRL). Panel (a) displays the most posterior section, while panel (f) the most anterior. Intervals between panels are 0.4 mm (a, b), 0.6 mm (b, c), 1.0 mm (c, d), 1.2 mm (d, e) and 1.0 mm (e, f). In panel (a), the medial pterygoid (PTmed) is fused with the lateral pterygoid (PTlat) at a site sandwiched by arrowheads. The former provides an upward protrusion (arrows in panel a). Posteriorly (panel d), the palatine bone (PAL) replaces the medial pterygoid (panels b and c) and approaches an ossified part of the ethmoid (ETH). The initial sphenoid sinus (SS) of this specimen is similar to that shown in Figure 9f: it is distant from the pterygoid and completely surrounded by the ethmoid (panels e and f). Panel (f) contains the future foramen sphenopalatinum through which the sphenopalatine artery runs to the nose. All panels are prepared at the same magnification (scale bar in panel a; 1 mm). Other abbreviations, see the common abbreviation

PTlat (Figures 6i, 7g, and 8g). Both during midterm and late-term, the medial PT muscle originated from the PTlat rather than the PTmed (Figures 6g, 7f, and 8g). Rather, the pharyngotympanic tube occupied a large space immediately posterior to the PTmed. The tensor veli palatini also attached to the PTlat rather than the PTmed (see the next subsection and Figure 10).

3.5 | Observations of late-term horizontal and frontal sections with a critical review of overall observations of sagittal sections

The present sagittal sections had a great advantage to show topographical relations among each elements of the developing sphenoid. However, they did not demonstrate three critical points of late-term morphologies: (1) the AP derivatives or a connection between the greater wing and BS; (2) the marginal parts of the greater wing membranous bones near the zygomatic bone as well as the squamous parts of the temporal, parietal, and frontal bones; (3) the uppermost part of the PT-med near or along the Vidian nerve. To make up for the weakness, we present horizontal and frontal sections from two of 25 specimens used for the previous study (Figures 10 and 11; see Section 2).

In horizontal sections, a suture along the greater wing margin was established with the temporal bone (Figure 10b insert) but not completed with the zygomatic bone (Figure 10a) as well as the parietal and frontal bones. The orbital muscle connected the maxilla with not only the greater wing (Figure 10c) but also zygomatic bone (Figure 10d,e). The muscle was also likely to attach to the posterior part (future lamina orbitalis) of the ethmoid (Figure 10b). Notably, a vertical bony plate of the PT-med protruded superiorly toward the AP (Figure 10b,c) and the latter provided a roof of the bony sphenoid canal. In contrast to the adult morphology, the PTmed and PTlat were connected in the middle or lower part (Figure 10f), not in the upper parts (Figure 10d).

Frontal sections also clearly demonstrated topographical relations among the PTmed, ethmoid, and palatine bone (Figure 11). The PTmed lay on the lateral aspect of the palatine bone vertical plate. The PT-med and PTlat were connected in the middle or lower part (Figure 11a). The palatine bone interposed between the PTmed and BS (Figure 11a–c). Moreover, at the upper end, the palatine bone attach not only to the BS (Figure 11a) but also to the initial concha sphenoidalis or the ossified parts of ethmoid (Figure 11d). The future foramen sphenopalatinum was seen between the palatine bone and ethmoid (Figure 11e). The initial concha as well as the cartilaginous ethmoid surrounded a deep upper recess of the nasal cavity or the initial sphenoid sinus (Figure 11e,f). Taken together with observations of horizontal sections, the bony AP provided a limited connection between the BS and greater wing (Figures 10a and 11a): this morphology was same as the early connection between the BS and cartilaginous AP and, even at later-term, the PTmed did not reach the BS.

4 | DISCUSSION

4.1 | Relationship of the prenatal sphenoid with morphology in adults

This study illustrated the entire developmental process of the sphenoid from embryos to late-term fetuses although sagittal sections had some disadvantage (see the final subsection of the Section 3). Figure 12 shows the relationship between each part of the adult sphenoid and its prenatal appearance. Derivative of the OS makes not only the lesser wing but also the anterior margin of the body of the sphenoid. Derivatives of the BS are the body of the sphenoid including the sella turcica and the dorsum sellae. Most of the greater wing including the foramen rotundum and the foramen oval originate from the AT and AP and multiple membranous bones. The PTmed process originated from endochondral bones and multiple membranous bones, while the lateral PT process derived from a single membranous bone. The AT was found to surround the maxillary nerve (i.e., the foramen rotundum) and to face the Vidian nerve (i.e., the sphenoid canal). Throughout the prenatal life, the AP connected the BS to the AT-derived greater wing. In contrast, the PT-med did not obtain a proper attachment to the BS before birth: they were separated by the ethmoid, palatine bone, and AP even at late-term. Likewise, the OS-derived lesser wing was still distant not only from the greater wing but also from the ethmoid and maxilla. Therefore, alongside the BS, paramedian parts of the late-term sphenoid was much thinner than the adult morphology.

Later-developing membranous bones are shown in pale colors in Figure 12, except that the sella turcica is shown in pale red on the superior view. It remains unclear whether a specific membranous bone belonged to the AT or PT because multiple membranous bones were continuous from the PTlat to the greater wing and because a cartilage core is not needed for membranous ossification. Nevertheless, to show the relationship between embryo and adult morphology, the various membranous bones were classified into those of the cartilaginous AT and AP and those of the PT. The pale green in the superomedial end of the PT seemed to be a membranous bone properly of the PT: its topographical anatomy was most difficult in the late-term sphenoid and, in addition to the sagittal sections, we needed observations of horizontal and frontal sections. The attachment of the palatine bone vertical plate to the concha sphenoidalis (Figure 11) was most likely to be absent in adults in spite of no or few available references.

Several parts require postnatal establishment. These include (1) an anterior end of the BS, including the concha sphenoidalis and the antero-inferior part of the sphenoidal canal; (2) a PTmed uppermost part connecting to the BS; (3) the inferolateral end and posterior margin of the greater wing (i.e., the bones around the foramen spinosum and adjacent to the parietal bone squamosal part and zygomatic bone); (4) the clinoid processes especially the anterior one; and (5) the lateral and inferior margins of the orbital fissure. Elongation of the clinoid processes seemed to require tension provided by dura-derived ligaments. The late-term large orbital fissure was largely closed by the orbital smooth muscle extending from the maxilla and ethmoid to membranous bones of the greater wing and zygomatic bone. Conversely, the greater wing was not attached to the OS, although both were connected to each other by a fibrous band at the orbital apex in late-term fetuses.

4.2 | Which of the present observations differed from previous descriptions?

Examination of these embryonic and fetal specimens detected several points differing from the classical concept. First, the OS did not

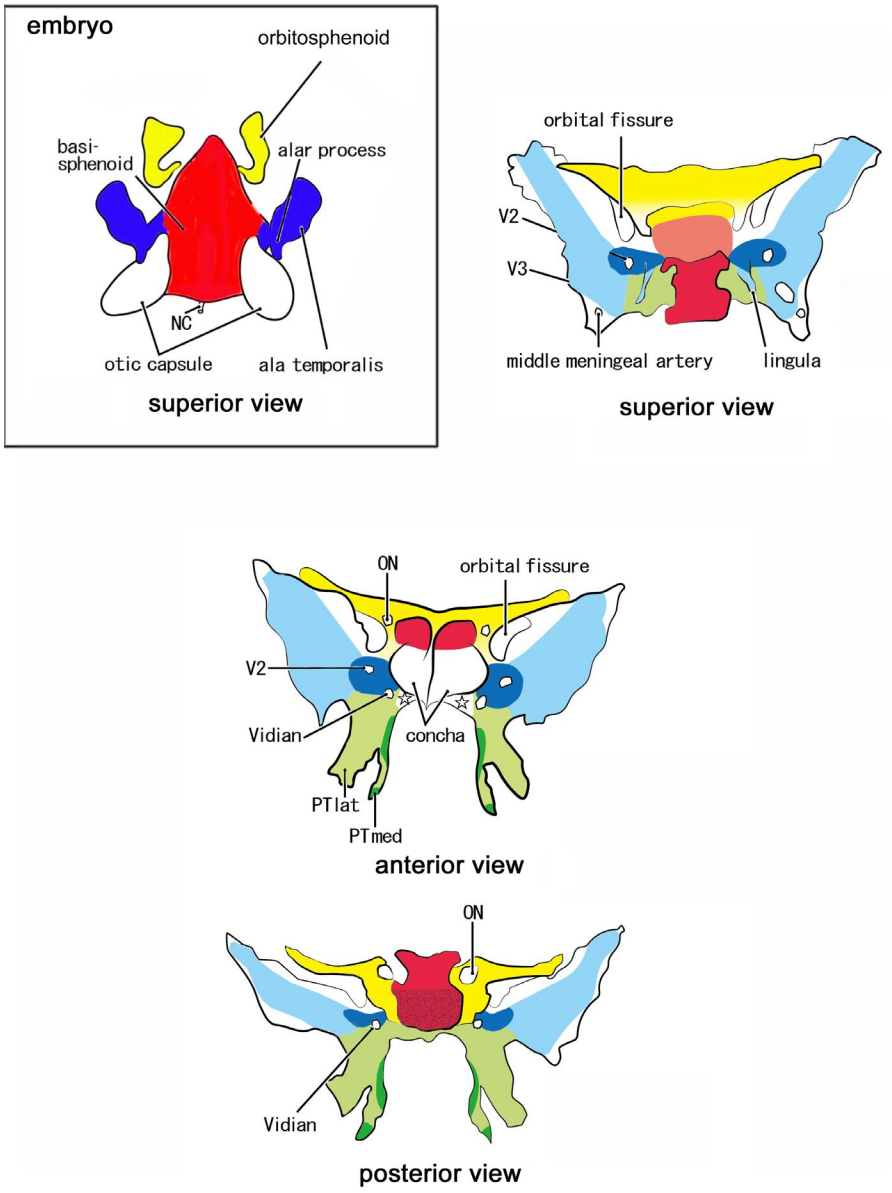

FIGURE 12 Schematic represenations to connect fetal elements of the sphenoid to the adult morphology. Embryo: Red color displays the basisphenoid (BS). Blue color exhibits the alar process (AP) and the ala temporalis (AT). Yellow color indicates the orbitosphenoid (OS). Adult: Red color displays derivatives of the BS: a pale-colored sella trucica in the superior view indicates the location deeper than the dorsum sellae. Blue color exhibits derivatives of the AT and AP: the pale blue indicates multiple membranous bones along and around the initial cartilages (dark blue). Green color shows the pterygoid: the limited dark green indicates endochondral bones for the hamulus and a marginal part of the medial pterygoid process (PTmed; anterior and posterior views). Yellow color indicates derivatives of the anterior, posterior, and superior bars of the OS. The OS makes not only the lesser wing but also a cartilage adjacent to the anterior margin of the BS (superior view). Star in the anterior view indicates a space occupied by the palatine bone and an ossified part of the ethmoid. ON, optic canal for the optic nerve; PTlat, lateral pterygoid process; V2, foramen rotundum for the maxillary nerve; V3, foramen ovale for the mandibular nerve; Vidian, sphenoid canal for the Vidian nerve

simply form a ring surrounding the optic nerve. Rather, two bars of the OS (i.e., the OSant and OSpost) initially sandwiched the optic nerve, with these parts later becoming connected at the inferolateral end to provide a superomedial bony margin of the orbital fissure. Guseva and Denisov (2006) seemed to be a limited available reference that described development changes in shape of the optic canal with a detailed morphometrical evaluation. They noted the shape similar to an hour-glass with "waists" (a narrow part of the canal). However, they did not have a view that the optic canal is built by multiple cartilages of the sphenoid.

Second, the anteromedial margins of the fetal sphenoid (the BS and lesser wing) in the classical concept showed a type of adult morphology despite the concha sphenoidalis being established postnatally. The anterior margin of the OSant+OSsup was not attached to the ethmoid but to the frontal bone. Moreover, fetal variations in the topographical relationships among the ethmoid, vomer, and palatine

bones around the initial sphenoid sinus suggested inter-individual differences in the contribution of the ethmoid to the definite concha.

Likewise, two points differed from the descriptions in Gray's Anatomy (Standling, 2005). Ossification was described as beginning at the root of the greater wing, below the foramen rotundum, at GA 8 weeks, with the first membranous ossification occurring in the PT below the foramen. In contrast, the first endochondral ossification was found to occur "above" the foramen rotundum. Gray's Anatomy also regards both PT-med and PTlat as being comprised of membranous bones, except for the hamulus. Indeed, the PTlat was formed by membranous bones along the AT inferior margin. However, the PTmed contained a single endochondral bone bar in addition to multiple membranous bones. Immunohistochemical analysis showed that the PT consisted of a mosaic of endochondral and membranous bones (Hayashi et al., 2014). In this context, a bony AP inserted into the cartilaginous AT corresponded to another type of "mosaic" or complex. Moreover, bones at multiple stages of endochondral ossification coexisted, as seen in the temporal bone petrosal portion of late-term fetuses (Honkura et al., 2020; Michaels et al., 2010). Finally, we did not find the lingula sphenoidalis although it was considered to ossify at 4 month along the lateral aspect of the internal carotid artery (see also the next subsection).

4.3 | Misunderstanding of and around the lingula sphenoidalis

The lingula sphenoidalis seemed to develop from the AP after birth. Actually, in late-term fetuses, we found a bony plate originating from the AP along the internal carotid artery. The intracavernous course of the internal carotid artery is almost straight in newborns and late-term fetuses (Sato et al., 2020; Weninger & Müller, 1999). The lingula might be a membranous bone formed by a mechanical stress to "bend" the parasellar artery after birth. Depending on growth of the skull base, the topographical relation among the BS, OSpost, and AP was likely to drastically change around the cavernous sinus. However, this later-developed membranous bone did not carry any ligament toward the mandible, resulting in a possible misunderstanding about this structure. In early fetuses, the sphenomandibular ligament, unconnected to the sphenoid, is continuous with the anterior ligament of the malleus, as both develop together from Meckel's cartilage (Rodríguez-Vázquez et al., 1992). At midterm, the anterior and sphenomandibular ligaments are continuous through the petrotympanic fissure (1992, 1998). At late-term, the sphenomandibular ligament originates from the petrotympanic fissure of the temporal bone, runs inferiorly on the immediately posterior side of the temporomandibular joint and lateral PT muscle and reaches the lingula mandibularis (figure 7 in Rodríguez-Vázquez et al., 2011; figure 2 in Katori, Yamamoto, et al., 2012). At all stages, the discomaleolar ligament is located near the sphenomandibular ligament; however, they differ because the former does not develop from Meckel's cartilage but independently in the lateral side (Rodriguez-Vázquez et al., 1993, 1998).

4.4 | Lesser wing elevation from the level of the hypophysis to a level higher than the ethmoid cribriform plate

At the beginning of this study, we had hypothesized that the orbital roof is elevated, depending on enlargement of the eye ball. However, the early roof, consisting of the cartilaginous OS and frontal bone, was found to have developed on the medial side of the eyeball, inasmuch as each eye is directed laterally rather than anteriorly. Thus, rapid inferior growth of the OSpost on the posterior side of the optic nerve was likely initially important for determining the height of the orbit. At early midterm, a connection was established between the cartilaginous OS and the bony frontal bone, with the latter bone keeping the orbital roof higher than the superior pole of the eyeball. Simultaneously, the maxilla occupied a large space below the eyeball, supporting and delineating the developing orbital content.

In contrast, the ethmoid was lower than the OS in early fetuses. Thus, the fetal orbital roof was transiently riding over the ethmoid cribriform plate. In late-term fetuses, a cartilage plate was found to extend anteriorly from the ossified OS and to pass over the frontal bone in the orbital roof. This plate seemed to provide an excess range of hard tissues to allow postnatal growth of the orbital roof. Captier et al., (2003) also noted the transient overlapped bony plates at the sphenofrontal suture. Therefore, the cartilaginous anterior part of the lesser wing was located on the superior side of the ethmoid and frontal bones, an arrangement that may allow a type of sliding during the rapid growth of the lesser wing. This sliding was likely dependent on the mechanical stress resulting from the expanding vault of the skull after birth. In contrast, the ossified posterior end of the ethmoid was fixed in the lower position by the nearby palatine bone, vomer, PTmed, and BS. In these anchors, the vomer was extremely bulky and developed early (Kim, Jin, et al., 2017; Kim, Oka, et al., 2017). Because of these anchors, the early ossified posterior part of the ethmoid seemed to be liable to separate from the major cartilaginous part depending on growth of the skull (see also above). Subsequently, a secondary fusion may occur between the BS and concha sphenoidalis.

4.5 | Fetal muscle attachments differ from those in adults

Two heads of the lateral PT muscle sandwich the buccal nerve after the upper head elongates to insert into the expanding greater wing (Katori, Kawase, et al., 2012). This change in muscle attachments may also apply to the medial PT muscle, with its origin extending from the PTlat, not the PT-med, to the greater wing. In this area, membranous bones were continuous between the PTlat and greater wing without any border. Thus, the muscle fibers anchored a superficial fibrous sheath of membranous bone, with membranous ossification occurring deep within the sheath. The former anchoring corresponds to the usual myotendinous junction, that is, a complex containing dystrophin and desmin (reviewed by Abe et al., 2010),

whereas the latter is the bone-tendon interface or enthesis, allowing sliding to occur between them. The medial PT insertion changed from Meckel's cartilage to the membranous bones that later cover the cartilage (Yamamoto & Abe, 2020; Yamamoto et al., 2020). In contrast to advanced molecular studies of the muscle-tendon-bone interface (Huang et al., 2015; Shukunami et al., 2006), to our knowledge, no information is available on the molecular basis of the changing muscle attachment.

The results of this study suggested differences in the origins of the extraocular muscles, with the superior rectus and obliquus superior originating from the OS-sup and the inferior and medial recti from the OSpost. This result was consistent with our previous studies in late-term fetuses and adults (Kim et al., 2020; Naito et al., 2019), which showed that the superior obliquus, levator palpebrae superioris, and superior rectus originated from the upper margin of the optic canal, whereas the other three recti arose from the medial wall of the fetal large orbital fissure (i.e., the OSpost). After birth, these origins may be connected or bundled by the future tendinous annulus.

4.6 | Molecular biology of the sphenoid differentiation and future perspectives

Assessment of the molecular control of the developing sphenoid in mice revealed a candidate signaling for differentiation of a combination between a limited element of the sphenoid and the other nearby bones. These included the PT and the first and second branchial arch skeletons in Hoxa-2 KO mice (Rijli et al., 1993) and the OS and the nasal capsule in mutant 3H1 *Br/Br* mice (McBratney et al., 2003). Similarly, we observed a histological fetal anomaly with an absent PT and OSpost (Jin et al., 2011). Conversely, each element of the cartilaginous sphenoid seemed not to be determined by a single signal. Moreover, the two types of fusion among the ossified BS, OS, and AT in human fetuses (Zhang et al., 2011) and between C57b and Balb-C mice (Yamamoto et al., 2020) suggest a redundancy in signaling. In contrast to cartilaginous elements, different paths of differentiation have been suggested for membranous ossified parts of the sphenoid. For example, in *Prox1* single mutant mice, membranous bones of the greater wing do not develop, with the maxilla and temporal bone squamosa replacing this area (ten Berg et al., 1998). Likewise, both Hedgehog and Wnt/beta-catenin signaling controls membranous bone differentiation around the AT and the PT (Xu et al., 2018).

Finally, in attempting to analyze cell lineage in mice, we found a gap between mouse and human sphenoid. Human BS was found to contain the notochord, whereas the mouse notochord disappears much earlier and at a much more posterior site than the human notochord. Most parts of the mouse sphenoid, including the BS, are of the neural crest origin, whereas the hypochismatic cartilage, possibly corresponding to the OS-post, is derived from the mesoderm (McBratney-Owen et al., 2008).

ACKNOWLEDGMENTS

This study was supported by Six Talent Peaks Project in Jiangsu province (SZCY-001) and a research project of Wuxi Commission of Health (Q201703) in China.

AUTHOR CONTRIBUTIONS

MY: correct data, and draft manuscript; ZWJ: correct and analysis data, manuscript editing, and funding acquisition; SH: analysis data, and manuscript writing; JFR: data collection, data analysis, and revise manuscript; GM: design study, data analysis, and revise manuscript; SA: data analysis and manuscript editing.

ORCID

Masahito Yamamoto https://orcid.org/0000-0001-9683-6678
Zhe-Wu Jin https://orcid.org/0000-0002-6789-2977
José Francisco Rodríguez-Vázquez https://orcid.org/0000-0001-5423-4492

REFERENCES

Abe, S., Rhee, S.-K., Osonoi, M., Nakamura, T., Cho, B.H., Murakami, G. et al. (2010) Expression of intermediate filaments at muscle insertions in human fetuses. *Journal of Anatomy*, 217, 167–173.

Captier, G., Cristol, R., Montoya, P., Prudhomme, M. & Godlewski, G. (2003) Prenatal organization and morphogenesis of the sphenofrontal suture in humans. *Cells Tissues Organs*, 175, 98–104.

Cho, K.H., Chang, H., Yamamoto, M., Abe, H., Rodríguez-Vázquez, J.F., Murakami, G. et al. (2013) Rathke's pouch remnant and its regression process in the prenatal period. *Childs Nervous System*, 29, 761–769.

Cho, K.H., Rodríguez-Vázquez, J.F., Han, E.H., Verdugo-López, S., Murakami, G. & Cho, B.H. (2010) Human primitive meninges in and around the mesencephalic flexure and particularly their topographical relation to cranial nerves. *Annals of Anatomy – Anatomischer Anzeiger*, 192, 322–328.

Fawcett, E. (1910) Note on the development of the human sphenoid. *Journal of Anatomy and Physiology*, 44, 207–222.

Guseva, Y.A. & Denisov, S.D. (2006) Structure of the optic canal in human ontogenesis. *Annals of Anatomy – Anatomischer Anzeiger*, 188, 103–116.

Hayashi, S., Kim, J.H., Hwang, S.E. et al. (2014) Interface between intramembranous and endochondral ossification in human fetuses. *Folia Morphol (Warsz)*, 73, 199–205.

Honkura, Y., Hayashi, S., Abe, H., Murakami, G., Rodríguez-Vázquez, J.F. & Shibata, S. (2020) The third vascular route of the inner ear or the canal of Cotugno: its topographical anatomy, fetal development and contribution to ossification of the otic capsule cartilage. *The Anatomical Record*, 304(4), 872–882. https://doi.org/10.1002/ar.24508

Honkura, Y., Takanashi, Y., Kawamoto-hirano, A.i., Abe, H., Osanai, H., Murakami, G. et al. (2017) Nasolacrimal duct opening to the inferior nasal meatus in human fetuses. *Okajimas Folia Anatomica Japonica*, 94, 101–108.

Honkura, Y., Yamamoto, M., Rodríguez-Vázquez, J.F., Murakam, G., Abe, H., Abe, S.-I. et al. (2021) Fetal development of the carotid canal with special reference to a contribution of the sphenoid bone and pharyngotympanic tube. *Anatomy & Cell Biology*, 54(2), 259–269.

Huang, A.H., Riordan, T.J., Pryce, B. et al. (2015) Musculoskeletal integration at the wrist underlies the molecular development of limb tendons. *Development*, 142, 2431–2441.

Jin, Z.W., Li, C.A., Kim, J.H., Shibata, S., Murakami, G. & Cho, B.H. (2011) Fetal head anomaly restricted to the eye, the mandible, and the pterygoid process of the sphenoid: a histological study. *Clinical Anatomy*, 24, 599–606.

Katori, Y., Kawamoto, A.I., Cho, K.H., Ishii, K., Abe, H., Abe, S. et al. (2013) Transsphenoidal meningocele: an anatomical study using human fetuses including report of a case. *European Archives of Oto-Rhino-Laryngology*, 270, 2729–2736.

Katori, Y., Kawase, T., Cho, K.H., Abe, H., Rodríguez-Vázquez, J.F., Murakami, G. et al. (2012) Prestyloid compartment of the parapharyngeal space: a histological study using late-stage human fetuses. *Surgical and Radiologic Anatomy*, 34, 909–920.

Katori, Y., Kawase, T., Ho Cho, K., Abe, H., Rodríguez-Vázquez, J.F., Murakami, G. et al. (2013) Suprahyoid neck fascial configuration, especially in the posterior compartment of the parapharyngeal space: a histological study using late-stage human fetuses. *Clinical Anatomy*, 26, 204–212.

Katori, Y., Yamamoto, M., Asakawa, M. et al. (2012) Fetal developmental change in topographical relation between the human lateral pterygoid muscle and buccal nerve. *Journal of Anatomy*, 220, 384–395.

Keibel, F. & Mall, F.P. (1910) *Manual of human embryology*. (Volume 1). Philadelphia, PA: J. B. Lippincott Company, pp. 427–429.

Kim, J.H., Hayashi, S., Yamamoto, M. et al. (2020) Examination of the annular tendon (Annulus of Zinn) as a common origin of the extraocular rectus muscles: 2. Embryological basis of extraocular muscle anomalies. *Investigative Ophthalmology & Visual Science*, 61, 5. https://doi.org/10.1167/iovs.61.12.5

Kim, J.H., Jin, Z.W., Shibata, S., Yang, J.D., Murakami, G., Rodríguez-Vázquez, J.F. et al. (2017a) Fetal development of human oral epithelial pearls with special reference to their stage-dependent changes in distribution. *Cleft Palate-Craniofacial Journal*, 54, 295–303.

Kim, J.H., Oka, K., Jin, Z.W., Murakami, G., Rodríguez-Vázquez, J.F., Ahn, S.W. et al. (2017b) Fetal development of the incisive canal, especially of the delayed closure: a study using serial sections of human fetuses. *Anatomical Record*, 300, 1093–1103.

Kiyokawa, H., Katori, Y., Cho, K.H., Murakami, G., Kawase, T. & Cho, B.H. (2012) Reconsideration of the autonomic cranial ganglia: an immunohistochemical study of midterm human fetuses. *Anatomical Record*, 295, 141–149.

McBratney, B.M., Margaryan, E., Ma, W., Urban, Z. & Lozanoff, S. (2003) Frontonasal dysplasia in 3H1 *Br/Br* mice. *Anatomical Record*, 271A, 291–302.

McBratney-Owen, B., Iseki, S., Bamforth, S.D., Olsen, B.R. & Morriss-Kay, G.M. (2008) Development and tissue origins of the mammalian cranial base. *Developmental Biology*, 322, 121–132.

Michaels, L., Soucek, S. & Linthicum, F. (2010) The intravestibular source of the vestibular aqueduct. II: its structure and function clarified by a developmental study of the intraskeletal channels of the otic capsule. *Acta Oto-Laryngologica*, 130, 420–428.

Naito, T., Cho, K.H., Yamamoto, M., Hirouchi, H., Murakami, G., Hayashi, S. et al. (2019) Examination of the topographical anatomy and fetal development of the tendinous annulus of Zinn for a common origin of the extraocular recti. *Investigative Opthalmology & Visual Science*, 60, 4564–4573.

Osanai, H., Abe, S., Rodríguez-Vázquez, J.F. et al. (2011) Human orbital muscle: a new point of view from the fetal development of extraocular connective tissue. *Investigative Ophthalmology & Visual Science*, 52, 1501–1506.

Rijli, F.M., Mark, M., Lakkaraju, S. et al. (1993) Homeotic transformation is generated in the rostral branchial region of the head by disruption of Hoza-2, which acts as a selector gene. *Cell*, 75, 1333–1349.

Rodríguez-Vázquez, J.F., Honkura, Y., Katori, Y., Murakami, G. & Abe, H. (2017) Fetal development of the pulley for muscle insertion tendons: a review and new findings related to the tensor tympani tendon. *Annals of Anatomy – Anatomischer Anzeiger*, 209, 1–10.

Rodríguez-Vázquez, J.F., Mérida-Velasco, J.R. & Jiménez-Collado, J. (1992) Development of the human sphenomandibular ligament. *Anatomical Record*, 233, 453–460.

Rodríguez-Vázquez, J.F., Mérida-Velasco, J.R. & Jiménez-Collado, J. (1993) Relationships between the temporomandibular joint and the middle ear in human fetuses. *Journal of Dental Research*, 72, 62–66.

Rodríguez-Vázquez, J.F., Mérida-Velasco, J.R., Mérida-Velasco, J.A. & Jiménez-Collado, J. (1998) Anatomical considerations on the discomalleolar ligament. *Journal of Anatomy*, 192, 617–621.

Rodríguez-Vázquez, J.F., Murakami, G., Verdugo-López, S. et al. (2011) Closure of the middle ear with special references to the development of the tegmen tympani of the temporal bone. *Journal of Anatomy*, 218, 690–698.

Sato, M., Cho, K.H., Yamamoto, M., Hirouchi, H., Murakami, G., Abe, H. et al. (2020) Cavernous sinus and abducens nerve in human fetuses near term. *Surgical and Radiologic Anatomy*, 42, 761–767.

Shukunami, C., Takimooto, A., Oro, M. et al. (2006) Scleraxis positively regulates the expression of tenomoduline, a differentiation marker od tenocytes. *Developmental Biology*, 298, 234–247.

Standling, S. (2005) *Gray's anatomy*, 39th edition. London: Elsevier Churchill Livingstone, pp. 467–468.

ten Berg, D., Brouwer, A., Korving, J. et al. (1998) *Prox1* and *Prox2* in skeletogenesis: roles in the craniofacial region, inner ear and limbs. *Development*, 125, 3831–3842.

Weninger, W.J. & Müller, G.B. (1999) The parasellar region of human infants: cavernous sinus topography and surgical approaches. *Journal of neurosurgery*, 90, 484–490.

Xu, R., Khan, S.K., Zhou, T. et al. (2018) G-alpha signaling controls intramembranous ossification during cranial bone development by regulating both Hedgehog and Wnt/beta-catenin signaling. *Bone Research*, 6, 33. https://doi.org/10.1038/s41413-018-0034-7.

Yamamoto, M., Abe, H., Hirouchi, H. et al. (2021) Development of the cartilaginous connecting apparatuses in the fetal sphenoid, with a focus on the alar process. *PLoS One*. in press.

Yamamoto, M. & Abe, S. (2020) Mechanism of muscle-tendon-bone complex development in the head. *Anatomical Science International*, 95, 165–173.

Yamamoto, M., Cho, K.H., Murakami, G. et al. (2018) Early fetal development of the otic and pterygopalatine ganglia with special reference to topographical relation with the developing sphenoid bone. *Anatomical Record*, 301, 1442–1453.

Yamamoto, M., Honkura, Y., Rodríguez-Vázque, J.F. et al. (2017) Morphology and relationships of ultimobranchial body with pharyngeal pouches. *European Journal of Anatomy*, 21, 119–124.

Yamamoto, M., Takada, H., Ishizuka, S., Kitamura, K., Jeong, J., Sato, M. et al. (2020) Morphological association between the muscles and bones in the craniofacial region. *PLoS One*, 15, e0227301. https://doi.org/10.1371/journal.pone.0227301.

Zhang, Q., Wang, H., Udagawa, J. et al. (2011) Morphological and morphometrical study on sphenoid and basioccipital ossification in normal human fetuses. *Congenital Anomalies*, 51, 138–148.

How to cite this article: Yamamoto, M., Jin, Z.-W., Hayashi, S., Rodríguez-Vázquez, J.F., Murakami, G. & Abe, S. (2021) Association between the developing sphenoid and adult morphology: A study using sagittal sections of the skull base from human embryos and fetuses. *Journal of Anatomy*, 239, 1300–1317. https://doi.org/10.1111/joa.13515